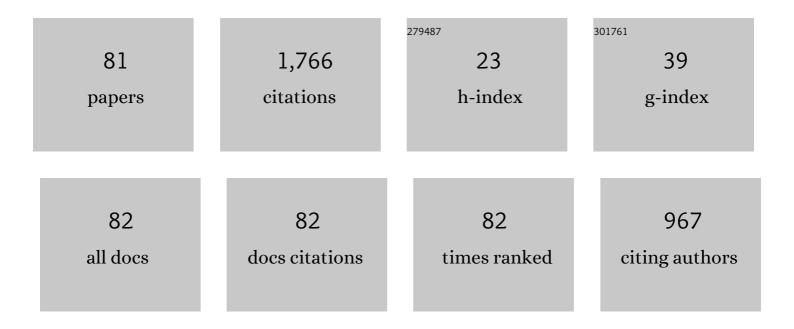
List of Publications by Year in descending order

Source: https://exaly.com/author-pdf/2765756/publications.pdf Version: 2024-02-01



ΜΙΛΟ-ΟΠΑΝΤΙ

#	Article	IF	CITATIONS
1	Diffusion bonding of dissimilar titanium alloys via surface nanocrystallization treatment. Journal of Materials Research and Technology, 2022, 17, 1274-1288.	2.6	12
2	Quantitative analysis of globularization and modeling of TC17 alloy with basketweave microstructure. Transactions of Nonferrous Metals Society of China, 2022, 32, 850-867.	1.7	4
3	The role of β phase in the morphology evolution of α lamellae in a dual-phase titanium alloy during high temperature compression. Journal of Alloys and Compounds, 2022, 910, 164901.	2.8	3
4	Further refinement mechanisms of nanograins in nanocrystalline surface layer of TC17 subjected to severe plastic deformation. Applied Surface Science, 2021, 538, 147941.	3.1	10
5	Effect of processing parameters on flow behaviors and microstructure during high temperature deformation of GH4586 superalloy. Journal of Central South University, 2021, 28, 338-350.	1.2	3
6	Quantitative characterization of β-solidifying γ-TiAl alloy with duplex structure. Transactions of Nonferrous Metals Society of China, 2021, 31, 1993-2004.	1.7	6
7	Twinning and twin intersections in γ grains of Ti-42.9Al-4.6Nb-2Cr. Journal of Materials Science and Technology, 2021, 88, 90-98.	5.6	12
8	Kinetic variables based constitutive model for high temperature deformation of Ti-46.5Al–2Nb–2Cr. Journal of Materials Research and Technology, 2021, 15, 3525-3537.	2.6	6
9	Interfacial Microstructure Characteristics and Mechanical Properties of a Press Bonded Ti–5Al–2Sn–2Zr–4Mo–4Cr Alloy. Crystals, 2021, 11, 1395.	1.0	0
10	Characteristics and formation mechanisms of defects in surface layer of TC17 subjected to high energy shot peening. Applied Surface Science, 2020, 509, 144711.	3.1	21
11	Kinetic analysis and strain-compensated constitutive models of Ti-42.9Al-4.6Nb–2Cr during isothermal compression. Progress in Natural Science: Materials International, 2020, 30, 260-269.	1.8	7
12	Sensitivity analysis on globularized fraction of α lamellae in titanium alloys. Transactions of Nonferrous Metals Society of China, 2019, 29, 305-312.	1.7	3
13	Microstructure evolution and its effect on flow stress of TC17 alloy during deformation in $\hat{I}_{\pm}+\hat{I}^2$ two-phase region. Transactions of Nonferrous Metals Society of China, 2019, 29, 1430-1438.	1.7	8
14	Characterization of crystal structure in the bonding interface between TC17 and TC4 alloys. Materials Characterization, 2019, 153, 169-174.	1.9	3
15	Dynamic Recrystallization-Related Interface Phase Boundary Migration of TC17/TC4 Bond with Initial Equiaxed Microstructure. Jom, 2019, 71, 2253-2261.	0.9	4
16	Structure response characteristics and surface nanocrystallization mechanism of alpha phase in Ti-6Al-4V subjected to high energy shot peening. Journal of Alloys and Compounds, 2019, 773, 860-871.	2.8	38
17	Prediction model for flow stress during isothermal compression in αÂ+Âβ phase field of TC4 alloy. Rare Metals, 2018, 37, 369-375.	3.6	5
18	Fragmentation of α Grains Accelerated by the Growth of β Phase in Ti–5Al–2Sn–2Zr–4Mo–4Cr during Hot Deformation. Advanced Engineering Materials, 2018, 20, 1700200.	1.6	3

#	Article	IF	CITATIONS
19	Evolution characterization of α lamellae during isothermal compression of TC17 alloy with colony-α microstructure. Materials Science & Engineering A: Structural Materials: Properties, Microstructure and Processing, 2018, 712, 637-644.	2.6	12
20	Grain size model for continuous dynamic recrystallization of titanium alloy in hot deformation. Science China Technological Sciences, 2018, 61, 1688-1695.	2.0	9
21	Deformation behavior and processing maps during isothermal compression of TC21 alloy. Rare Metals, 2017, 36, 86-94.	3.6	10
22	Metadynamic recrystallization of 300M steel after isothermal compression. Materials at High Temperatures, 2017, 34, 279-288.	0.5	6
23	Constitutive model and optimal processing parameters of TC17 alloy with a transformed microstructure via kinetic analysis and processing maps. Materials Science & Engineering A: Structural Materials: Properties, Microstructure and Processing, 2017, 698, 302-312.	2.6	34
24	Influence of pressure on interfacial microstructure evolution and atomic diffusion in the hot-press bonding of Ti-33Al-3V to TC17. Journal of Alloys and Compounds, 2017, 720, 131-138.	2.8	22
25	Prediction model for surface layer microhardness of processed TC17 via high energy shot peening. Transactions of Nonferrous Metals Society of China, 2017, 27, 1956-1963.	1.7	3
26	Nanostructure and surface roughness in the processed surface layer of Ti-6Al-4V via shot peening. Materials Characterization, 2017, 123, 83-90.	1.9	76
27	Nanocrystallization mechanism of beta phase in Ti-6Al-4V subjected to severe plastic deformation. Materials Science & Engineering A: Structural Materials: Properties, Microstructure and Processing, 2016, 669, 7-13.	2.6	45
28	Stress-induced twinning of nanocrystalline hexagonal close-packed titanium in Ti-6Al-4V. Materials Letters, 2016, 180, 47-50.	1.3	11
29	Plastic flow behavior of superalloy GH696 during hot deformation. Transactions of Nonferrous Metals Society of China, 2016, 26, 712-721.	1.7	10
30	Deformation mechanisms of nanocrystalline alpha titanium in Ti-6Al-4V. Materials Letters, 2016, 185, 488-490.	1.3	16
31	Evolution mechanisms of the primary α and β phases during α/β deformation of an α/β titanium alloy TC8. Materials Characterization, 2016, 120, 115-123.	1.9	27
32	Three-dimensional Numerical Simulation and Experimental Analysis of Austenite Grain Growth Behavior in Hot Forging Processes of 300M Steel Large Components. Journal of Iron and Steel Research International, 2016, 23, 1012-1019.	1.4	6
33	Formation of adiabatic shear band and deformation mechanisms during warm compression of Ti–6Al–4V alloy. Rare Metals, 2016, 35, 598-605.	3.6	5
34	Surface nanocrystallization and gradient structure developed in the bulk TC4 alloy processed by shot peening. Journal of Alloys and Compounds, 2016, 685, 186-193.	2.8	87
35	Significance and interaction of bonding parameters with bonding ratio in press bonding of TC4 alloy. Rare Metals, 2016, 35, 235-241.	3.6	5
36	Detailed Evolution Mechanism of Interfacial Void Morphology in Diffusion Bonding. Journal of Materials Science and Technology, 2016, 32, 259-264.	5.6	32

#	Article	IF	CITATIONS
37	High Temperature Behavior of Isothermally Compressed M50 Steel. Journal of Iron and Steel Research International, 2015, 22, 969-976.	1.4	6
38	Bonding interface characteristic and shear strength of diffusion bonded Ti-17 titanium alloy. Transactions of Nonferrous Metals Society of China, 2015, 25, 80-87.	1.7	28
39	Quantitative analysis on microstructure evolution of Ti-6Al-2Zr-2Sn-2Mo-1.5Cr-2Nb alloy during isothermal compression. Rare Metals, 2015, 34, 625-631.	3.6	4
40	Microstructure and mechanical properties of heat-treated Ti–5Al–2Sn–2Zr–4Mo–4Cr. Transactions of Nonferrous Metals Society of China, 2015, 25, 2893-2900.	1.7	19
41	The gradient crystalline structure and microhardness in the treated layer of TC17 via high energy shot peening. Applied Surface Science, 2015, 357, 197-203.	3.1	55
42	The modelling of dynamic recrystallization in the isothermal compression of 300M steel. Materials Science & Engineering A: Structural Materials: Properties, Microstructure and Processing, 2013, 574, 1-8.	2.6	69
43	Modeling of void closure in diffusion bonding process based on dynamic conditions. Science China Technological Sciences, 2012, 55, 2420-2431.	2.0	38
44	Variation effect of strain rate on microstructure in isothermal compression of Ti-6Al-4V alloy. Rare Metals, 2012, 31, 7-11.	3.6	8
45	3D finite element simulation of microstructure evolution in blade forging of Ti-6Al-4V alloy based on the internal state variable models. International Journal of Minerals, Metallurgy and Materials, 2012, 19, 122-130.	2.4	6
46	Lattice variations of Ti-6Al-4V alloy with hydrogen content. Materials Characterization, 2011, 62, 724-729.	1.9	27
47	The growth behavior of austenite grain in the heating process of 300M steel. Materials Science & Engineering A: Structural Materials: Properties, Microstructure and Processing, 2011, 528, 4967-4972.	2.6	109
48	Optimization of TC11 alloy forging parameters using processing maps. Rare Metals, 2011, 30, 222-226.	3.6	9
49	Modeling of grain size in isothermal compression of Ti-6Al-4V alloy using fuzzy neural network. Rare Metals, 2011, 30, 555-564.	3.6	8
50	Effect of hydrogen addition on the microstructure of TC21 alloy. Materials Science & Engineering A: Structural Materials: Properties, Microstructure and Processing, 2010, 527, 7080-7085.	2.6	15
51	Microstructure evolution in the high temperature compression of Ti-5.6Al-4.8Sn-2.0Zr alloy. Rare Metals, 2010, 29, 533-537.	3.6	6
52	Thermomechanical coupling simulation and experimental study in the isothermal ECAP processing of Ti-6Al-4V alloy. Rare Metals, 2010, 29, 613-620.	3.6	8
53	Microscopic characterization of semi-solid aluminium alloys. International Journal of Minerals, Metallurgy and Materials, 2010, 17, 290-296.	2.4	4
54	High-Temperature Deformation Behavior of Ti-6Al-4V Alloy without and with Hydrogenation Content of 0.27 wt.%. Journal of Materials Engineering and Performance, 2010, 19, 59-63.	1.2	7

#	Article	IF	CITATIONS
55	Deformation Behavior and Constitutive Equation Coupled the Grain Size of Semi-Solid Aluminum Alloy. Journal of Materials Engineering and Performance, 2010, 19, 1337-1343.	1.2	5
56	Constitutive model for high temperature deformation of titanium alloys using internal state variables. Mechanics of Materials, 2010, 42, 157-165.	1.7	122
57	Prediction of flow stress in isothermal compression of Ti–6Al–4V alloy using fuzzy neural network. Materials & Design, 2010, 31, 3078-3083.	5.1	15
58	FE-based coupling simulation of Ti60 alloy in isothermal upsetting process. Transactions of Nonferrous Metals Society of China, 2010, 20, 849-856.	1.7	3
59	Effect of the strain on the deformation behavior of isothermally compressed Ti–6Al–4V alloy. Materials Science & Engineering A: Structural Materials: Properties, Microstructure and Processing, 2009, 505, 88-95.	2.6	83
60	Effect of 0.16wt% hydrogen addition on high temperature deformation behavior of the Ti600 titanium alloy. Materials Science & Engineering A: Structural Materials: Properties, Microstructure and Processing, 2009, 513-514, 228-232.	2.6	21
61	Application of Thermohydrogen Processing for Formation of Ultrafine Equiaxed Grains in Near α Ti600 Alloy. Metallurgical and Materials Transactions A: Physical Metallurgy and Materials Science, 2009, 40, 3009-3015.	1.1	11
62	Effect of hydrogenation on the microstructure of Ti-5.6Al-4.8Sn-2.0Zr alloy. Rare Metals, 2009, 28, 343-345.	3.6	0
63	Effect of Processing Parameters on Microstructure and Mechanical Properties in High Temperature Deformation of Ti-6Al-4V Alloy. Rare Metal Materials and Engineering, 2009, 38, 19-24.	0.8	27
64	Effect of the strain on processing maps of titanium alloys in isothermal compression. Materials Science & Engineering A: Structural Materials: Properties, Microstructure and Processing, 2009, 504, 90-98.	2.6	52
65	Effect of 0.770wt%H addition on the microstructure of Ti–6Al–4V alloy and mechanism of δ hydride formation. Journal of Alloys and Compounds, 2009, 481, 480-485.	2.8	42
66	High temperature deformation behavior of a near alpha Ti600 titanium alloy. Materials Science & Engineering A: Structural Materials: Properties, Microstructure and Processing, 2008, 492, 24-28.	2.6	88
67	Internal state variable models for microstructure in high temperature deformation of titanium alloys. Science in China Series D: Earth Sciences, 2008, 51, 1921-1929.	0.9	2
68	Microstructure and Element Distribution during Partial Remelting of an Al-4Cu-Mg alloy. Journal of Materials Engineering and Performance, 2008, 17, 25-29.	1.2	7
69	Effect of hydrogenation content on high temperature deformation behavior of Ti–6Al–4V alloy in isothermal compression. International Journal of Hydrogen Energy, 2008, 33, 2714-2720.	3.8	35
70	Modeling of constitutive relationships and microstructural variables of Ti–6.62Al–5.14Sn–1.82Zr alloy during high temperature deformation. Materials Characterization, 2008, 59, 1386-1394.	1.9	21
71	Grain refinement in near alpha Ti60 titanium alloy by the thermohydrogenation treatment. International Journal of Hydrogen Energy, 2007, 32, 626-629.	3.8	30
72	High temperature deformation behavior of near alpha Ti–5.6Al–4.8Sn–2.0Zr alloy. Journal of Materials Processing Technology, 2007, 183, 71-76.	3.1	81

#	Article	IF	CITATIONS
73	Deformation Behavior in the Isothermal Compression of Hydrogenated Ti–5.6Al–4.8Sn–2.0Zr–1.0Mo Alloy. Journal of Materials Engineering and Performance, 2007, 16, 93-96.	1.2	8
74	A set of microstructure-based constitutive equations in hot forming of a titanium alloy. International Journal of Minerals, Metallurgy, and Materials, 2006, 13, 435-441.	0.2	8
75	Finite Element Simulation of Deformation Behavior in Friction Welding of Al-Cu-Mg Alloy. Journal of Materials Engineering and Performance, 2006, 15, 627-631.	1.2	13
76	Acquiring a Novel Constitutive Equation of a TC6 Alloy at High-Temperature Deformation. Journal of Materials Engineering and Performance, 2005, 14, 263-266.	1.2	8
77	Deformation Behavior of TC6 Alloy in Isothermal Forging. Journal of Materials Engineering and Performance, 2005, 14, 671-676.	1.2	12
78	Microscopic observation of cold-deformed Al–4Cu–Mg alloy samples after semi-solid heat treatments. Materials Characterization, 2005, 54, 451-457.	1.9	22
79	Deformation behavior and microstructural evolution during the semi-solid compression of Al–4Cu–Mg alloy. Materials Characterization, 2005, 54, 423-430.	1.9	19
80	Fabrication and Microstructure Evolution of Semi-Solid LY11 Alloy by SIMA. Journal of Materials Engineering and Performance, 2003, 12, 249-253.	1.2	8
81	Microstructural evolution and modelling of the hot compression of a TC6 titanium alloy. Materials Characterization, 2002, 49, 203-209.	1.9	33